Case Studies in Thermal Engineering 21 (2020) 100706

Contents lists available at ScienceDirect

Case Studies in Thermal Engineering

journal homepage: http://www.elsevier.com/locate/csite

Numerical heat transfer analysis & predicting thermal performance of fins for a novel heat exchanger using machine learning

Gaurav Krishnayatra *, Sulekh Tokas, Rajesh Kumar

Department of Mechanical Engineering, Delhi Technological University, Delhi, India

ARTICLE INFO

Keywords:
Convection heat transfer
Fin effectiveness
Fin efficiency
Novel fins
Machine learning
K-nearest neighbor

ABSTRACT

In the present case study, the thermal performance of fins for a novel axial finned-tube heat exchanger is investigated and predicted using machine learning regression technique. The effects of variation in the fin spacing, fin thickness, material, and the convective heat transfer coefficient on the overall efficiency and total effectiveness have been analyzed and commented upon. The *k*-Nearest Neighbor (*k*-NN), a machine learning algorithm, is used for regression analysis to predict the thermal performance outputs and the results showed high prediction accuracies. The *k*-NN algorithm is robust and precise which can be used by thermal system design engineers for predicting output variables. The temperature profiles of various geometries have been depicted and compared in the results. It was concluded that the efficiency is increasing with fin thickness & decreasing with fin spacing and the maximum efficiency $\eta_{max} = 0.99975$ is achieved at $\delta^* = 0.1$ & $t^* = 0.0133$ having $h = 5\ W/m^2.K$ for copper material. The effectiveness is increasing with fin spacing & fin thickness and the maximum effectiveness $\varepsilon_{max} = 122.766$ is for $\delta^* = 8$ & $t^* = 0.4$ having $h = 5\ W/m^2.K$.

1. Introduction

Extended surfaces (fins) are widely employed in various heat transfer components used in a wide range of applications like heat sinks, microprocessor cooling & latent thermal energy storage devices [1,2] and thus the fins have always been a notable domain for research. Increasing the exposed surface area by employing the fins is a prominent method to enhance the rate of heat transfer with the advantage of being economically feasible. Extensive studies are available which analyze the thermal performance and costing of different types of fins. Harper and Brown [3] presented two-dimensional analytical solutions for circumferential and longitudinal fins having rectangular and wedge type shape. It was deduced that the one-dimensional model is sufficient to evaluate the performance of the fin. Schmidt [4] examined the performance of various profiles for longitudinal fins and concluded that the parabolic profile is the optimum type of profile for longitudinal fins. Heggs & Ooi [5] evaluated the performance of radial rectangular fins and presented variations in thermal performance for different designs. Alam & Ghoshdastidar [6] performed numerical study using FDM on a circular tube with internal longitudinal fins having a tapered lateral profile, it was observed that there is a significant improvement in the net heat transfer rate with the installation of fins. Nagarani et al. [7] performed optimization using genetic algorithm on the geometrical parameters of the elliptical annular fin (EAF). The result showed that the EAF is more effective than the conventional circular fin for a

* Corresponding author.
E-mail address: gauravkrishnayatra_mt2k18@dtu.ac.in (G. Krishnayatra).

https://doi.org/10.1016/j.csite.2020.100706
Received 3 June 2020; Received in revised form 25 June 2020; Accepted 27 June 2020
Available online 4 July 2020

fixed cross-sectional area irrespective of the efficiency when the shape factor (SF) is less than 0.5. Cuce & Cuce [8] used CFD to investigate the performance of novel rectangular fin designs with single-step change (RFSSC) and double-step change (RFDSC). The RFSSC fins were found to be more efficient than the conventional rectangular fin (CRF). Aziz and Khani [9] developed analytical solutions to examine the performance of rectangular and various convex parabolic fins installed on a rotating shaft using homotopy analysis method (HAM). The highest rate of heat transfer was recorded for uniform fin thickness and the effectiveness increased with the rotational speed of the shaft. Okiy [10] investigated the effect of two-dimensional heat transfer in radial and planar fins in comparison to the assumption of one-dimensional heat transfer in fin analysis. It was concluded that one-dimensional heat transfer assumption provided inaccurate solutions with respect to two-dimensional heat transfer for short planar fins. Samana et al. [11] experimentally examined the fin efficiency of a solid wire fin used in a wire-on-tube heat exchanger and the fin efficiency increased with the use of oscillating heat pipe in comparison to solid wire fin. Li et al. [12] performed experiments to study the effects of various thermal boundary conditions and thermal conductivity on the thermal performance of a pin fin array using liquid crystal sheet, and it was concluded that thermal conductivity is directly influencing the rate of heat transfer.

After a thorough literature review, it was deduced that some designs of finned-tube heat exchangers are particularly overlooked and many studies have utilized the artificial neural network [13,14] however, very limited studies have utilized the *k*-Nearest Neighbor for regression analysis. A novel type of fins is designed and its thermal performance has been analyzed in this computational investigation. The finned-tube heat exchanger consists of a hollow tube with an isothermal boundary condition at the inner wall (in order to simulate some of the industrial applications) having the novel rectangular fins attached axially at the outer wall. The novel design of fins consists of a fin-on-fin approach, where in Fig. 1 it is visible that the tube has primary fins (colored in black), this is a simple case of longitudinal fins attached to the outer surface of the tube. But consequently another set of fins, the secondary fins (colored in blue), are attached on to the primary fins in order to increase the total finned area that proportionately enhance the total rate of heat transfer. In this study, the variations of the overall Efficiency and the Effectiveness of the novel finned-tube system has been analyzed with respect to the varying fin thickness, fin spacing, material of the system, and the convective heat transfer coefficient using Ansys Fluent. Moreover, Machine learning technique called *k*-Nearest Neighbor (*k*-NN) has been employed for regression analysis to predict the thermal performance of the novel finned-tube system.

2. Physical model & governing equations

The design consists of a tube with the inner diameter (D_i) and the outer diameter (D_o) of 5 & 6 mm respectively with the fin thickness (t) being varied from 0.2 to 2.4 mm and having the fin spacing (δ) from 0.6 to 48 mm as shown in Fig. 1. The two materials of the finned-tube system chosen are Copper ($K_{cu} = 387.6\ W/m.K$) and Steel ($K_{ss} = 16.7\ W/m.K$). The conjugated heat transfer is taking place from the inner isothermal wall ($T_w = 400\ K$) to the ambient air ($T_\infty = 300\ K$). To reduce computational cost and time, the simulated flow of air on the outer surface of the finned-tube system has not been considered. However, a range of convective heat transfer coefficient has been taken which covers almost all the practical applicated values found in heat exchangers in order to visualize the impact of its variation on the efficiency and the effectiveness of the system. The convective heat transfer coefficient (h) at the outer surface is being varied from 5 to 200 W/m^2.K.

The governing partial differential equations used to solve the conjugated heat transfer problem are linearized and computed in the Ansys Fluent using with the following assumptions.

1. The material is homogenous and isotropic.
2. The fin tips are adiabatic.
3. The convective heat transfer coefficient is uniform over the entire outer surface area.
4. The radiation phenomenon is neglected.

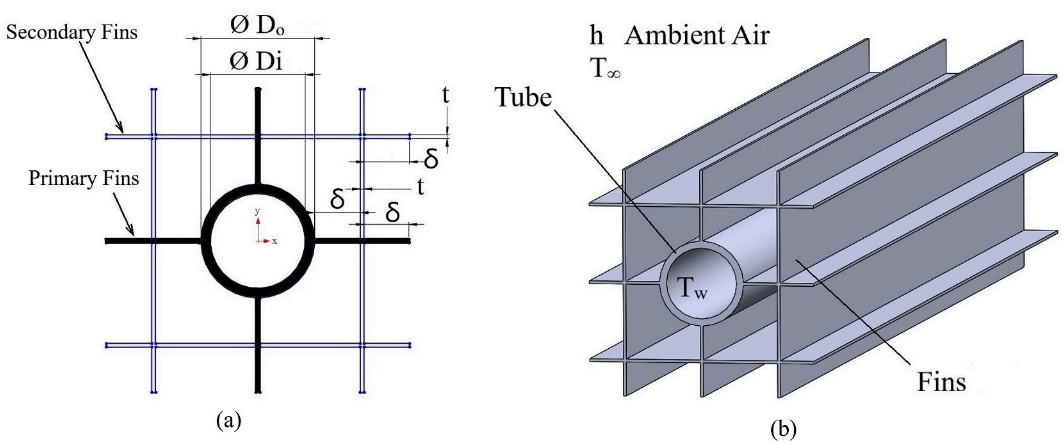

Fig. 1. a) Schematic model of the novel finned-tube heat exchanger b) 3-Dimensional Representation of the model.

The energy equation for the finned-tube system [1]:

$$\left\{\frac{d^2T}{dx^2}+\frac{d^2T}{dy^2}\right\}=0 \tag{1}$$

The heat transfer equation for the outer surface [1]:

$$Q=\frac{(T_w-T_\infty)}{\frac{\ln\left(D_o/D_i\right)}{2\pi kL}+\frac{1}{\eta_o A_t h}} \tag{2}$$

Where, k is the thermal conductivity of the material, h is the convective heat transfer coefficient and η_o is the overall efficiency of the finned-tube [1].

$$\eta_o=1-\frac{NA_f}{A_t}\left(1-\eta_f\right) \tag{3}$$

Where, η_f is the efficiency of a single fin, A_f the surface area of single fin and A_t the total surface area of the finned-tube system. The total surface area of the novel finned-tube system is calculate by:

$$A_t=L_{exp}\times L \tag{4}$$

$$L_{exp}=48\delta+8(D_o-t) \tag{5}$$

Where, axial length (L) of the system is unity and L_{exp} is the total perimetric length of the outer surface of the novel finned-tube system.

Equations (2) and (3) are used to validate the computational results for a simple finned-tube system having 4 equidistant axial fins attached at the outer surface of a hollow tube having same diameters with fin length $L_f=10\ mm$ and fin thickness $t=0.5\ mm$ as shown in Fig. 2 along with the heat flux variation with convective heat transfer coefficient which is showing remarkable agreement.

The overall Efficiency for the system is given as:

$$\eta=\frac{q}{h(T_w-T_\infty)} \tag{6}$$

Where, q is the area weighted average of the heat flux at the outer surface of the novel finned-tube system computed from the simulations. And the total effectiveness of the system is:

$$\varepsilon=\frac{Q}{hA_o(T_w-T_\infty)} \tag{7}$$

Where, Q is the area surface integral of the heat flux at the outer surface computed by simulation.

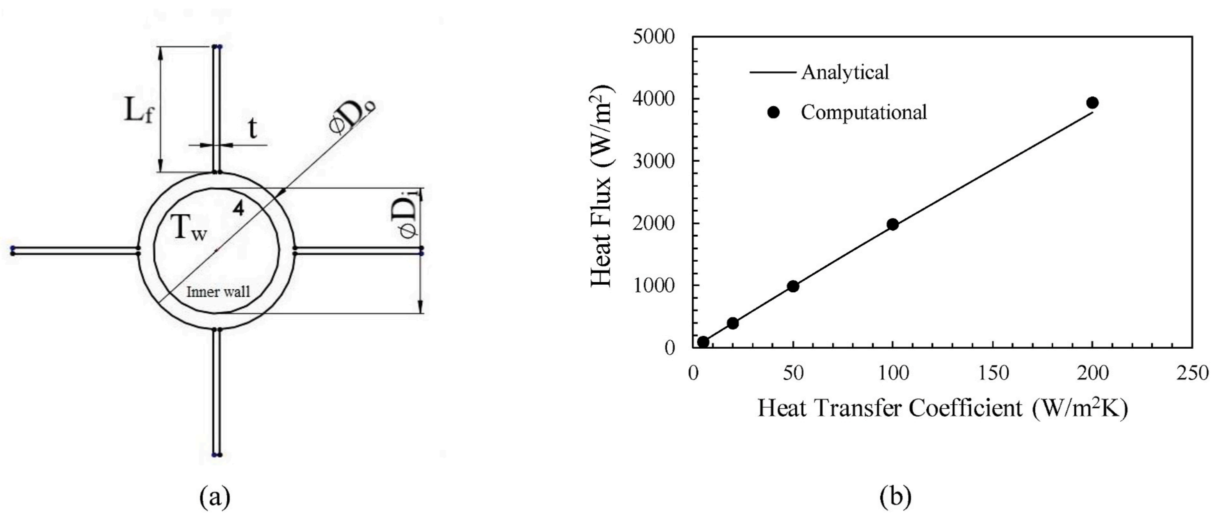

Fig. 2. a) Schematic finned-tube system used for convective heat transfer validation with 4 axial fins at the outer surface of the tube b) Variation of heat flux with convective heat transfer coefficient representing the comparing between analytical and computational heat flux values.

3. Computational & machine learning modelling

3.1. Computational modelling

A 2-Dimensional analysis is performed in this study in order to reduce the computational time. Moreover, the 2D model of the finned-tube system is symmetrical about 4 axes, therefore the $1/8^{th}$ 2D model is selected for the study as shown in Fig. 3. The 2D models were developed using Solidworks software and then were modeled & solved in Ansys Fluent. The models were discretized into a finite number of control volumes on which the governing equations were solved using appropriate approximations. Second-order upwind was used for energy equation and the residual value was set to 10^{-9}. Tetrahedron meshing was done on the solid domain as shown in Fig. 3 and the mesh convergence test was also performed to make the result independent of the size of the elements. Table 1 is showing the variation of heat flux with the element size and it can be inferred that the heat flux is getting independent when the size of the element is at 0.0125 mm.

3.2. Machine learning modelling

This section explains the utilization of supervised machine learning technique called *k*-Nearest Neighbor (*k*-NN) which has been applied as a regression tool [15]. The *k*-NN algorithm is robust, precise and computationally fast when used as a regression model, moreover it works well with a fewer number of input variables and relatively small data set which is used in designing of thermal systems. The dataset for the regression analysis is procured from the simulations result for all the geometries considered in the study, the dataset includes the output variables namely the efficiency (η) & the effectiveness (ε) of the finned-tube heat exchanger and the outer diameter of tube (D_o), fin spacing (δ), fin thickness (t), thermal conductivity of the material (k), and the convective heat transfer coefficient (h) are the input variables. Therefore, the variables are represented in the forms of following functions.

$$\eta = f_1(D_o, \delta, t, k, h) \tag{8}$$

$$\varepsilon = f_2(D_o, \delta, t, k, h) \tag{9}$$

In order to dimensionally balance the equation, the input variables are converted into non-dimensional forms subsequently decreasing the number of input variables.

$$\eta = f_3(\delta^*, t^*, M) \tag{10}$$

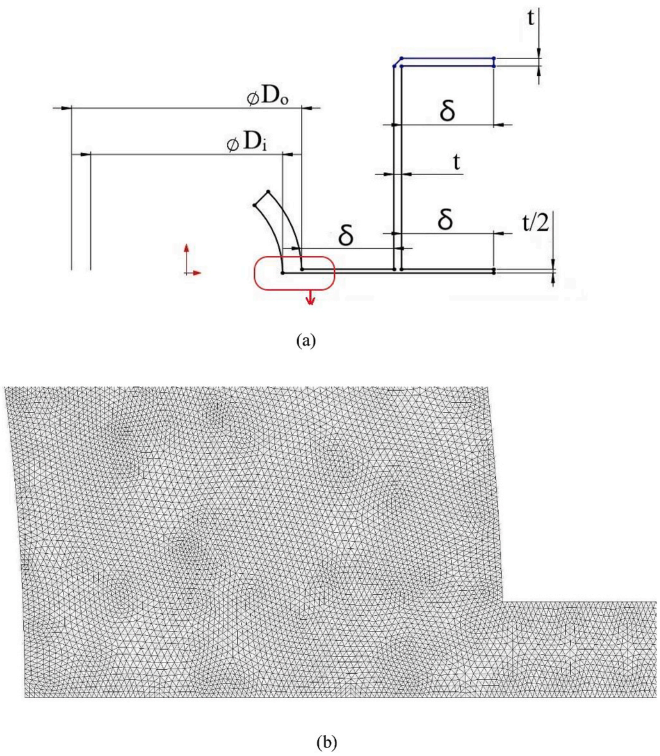

Fig. 3. a) $1/8^{th}$ model designed for the simulation b) The red encircled portion of the $1/8^{th}$ model is shown after descritization

Table 1
Variation of heat flux with number of elements and element size.

Max. Element Size (mm)	Number of Elements	Heat Flux $q(W/m^2)$	Difference in q (%)
0.05	31392	498.187	0.212
0.04	51936	497.129	1.913
0.03	96128	487.796	2.154
0.02	191072	498.536	-0.266
0.015	344592	497.210	0.057
0.0125	461472	497.494	-0.012
0.01	601844	497.555	–

$$\varepsilon = f_4(\delta^*,\ t^*,\ M) \tag{11}$$

Where, δ^* is the non-dimensional fin spacing, t^* is the non-dimensional fin thickness and M is a new non-dimensional parameter used for this study, relations given below:

$$\delta^* = \frac{\delta}{D_o} \tag{12}$$

$$t^* = \frac{t}{D_o} \tag{13}$$

$$M = \frac{h}{8k} L_{exp} \tag{14}$$

The k-NN algorithm is a “black-box” regression tool where the actual functions are not derived instead they are predicted from the dataset. The dataset is divided into two parts: 65% Testing data & 35% Training data, the training dataset is used for “learning” and the testing dataset is used for validating the predictions with actual output values. The prediction accuracy of k-NN regression is calibrated by two factors namely, the “k” number of close neighbors and the type of metric distance between the outputs [16]. In Fig. 4, the output y_i is scattered with respect to the inputs x_i & z_i for $k = 3$ number of neighbors. The p_i is the prediction computed on the basis of the median of Euclidean distances $(d_{12},\ d_{13}\ \&\ d_{14})$ of y_1 from $y_2,\ y_3\ \&\ y_4$, which are the 3 closest neighboring outputs. The Euclidean distance is calculated by

$$d_{ij} = \sqrt{(x_i - x_j)^2 + (z_i - z_j)^2} \tag{15}$$

Where, d_{ij} calculates the Euclidean distance between the ith and jth elements in the input data.

The predicted values of the outputs are compared to the computed outputs from the simulation results in terms of R^2 values to check the accuracy of the regression model and the selection of “k” is based on the accuracy of the regression model. The R^2 value is the

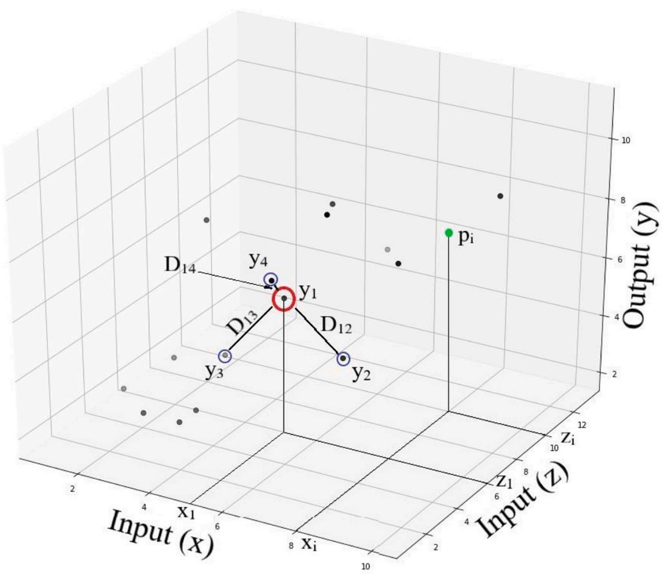

Fig. 4. Three-Dimensional scattering of output variable shown with variation of inputs 1 & 2 for $k = 3$ number of neighbors.

coefficient of determination which is given by the following relation.

$$R^2 = 1 - \frac{\sum_i (y_i - p_i)^2}{\sum_i (y_i - \bar{y})^2} \tag{16}$$

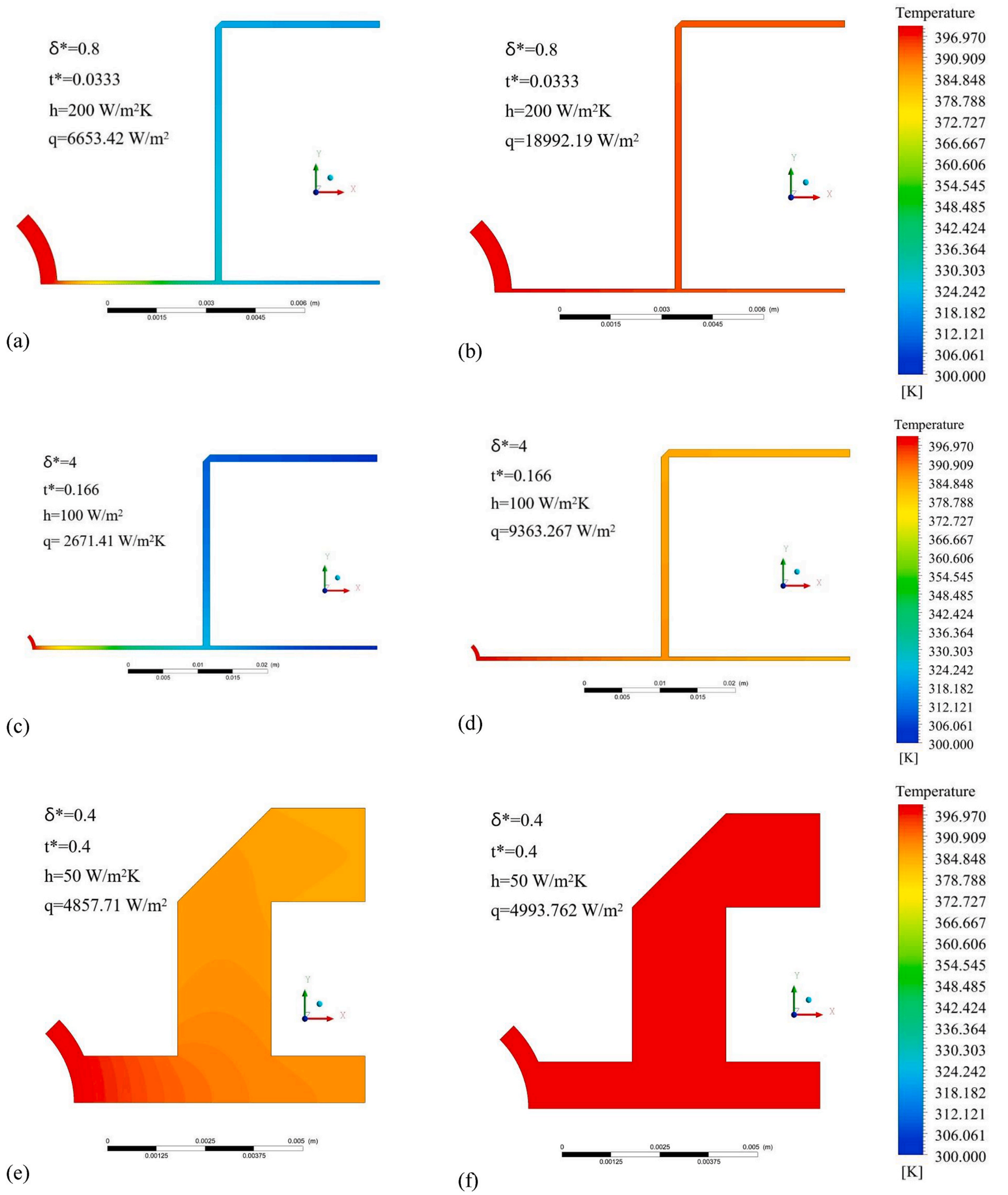

Fig. 5. Temperature plumes of cross-section for different geometries and different convective heat transfer coefficients.

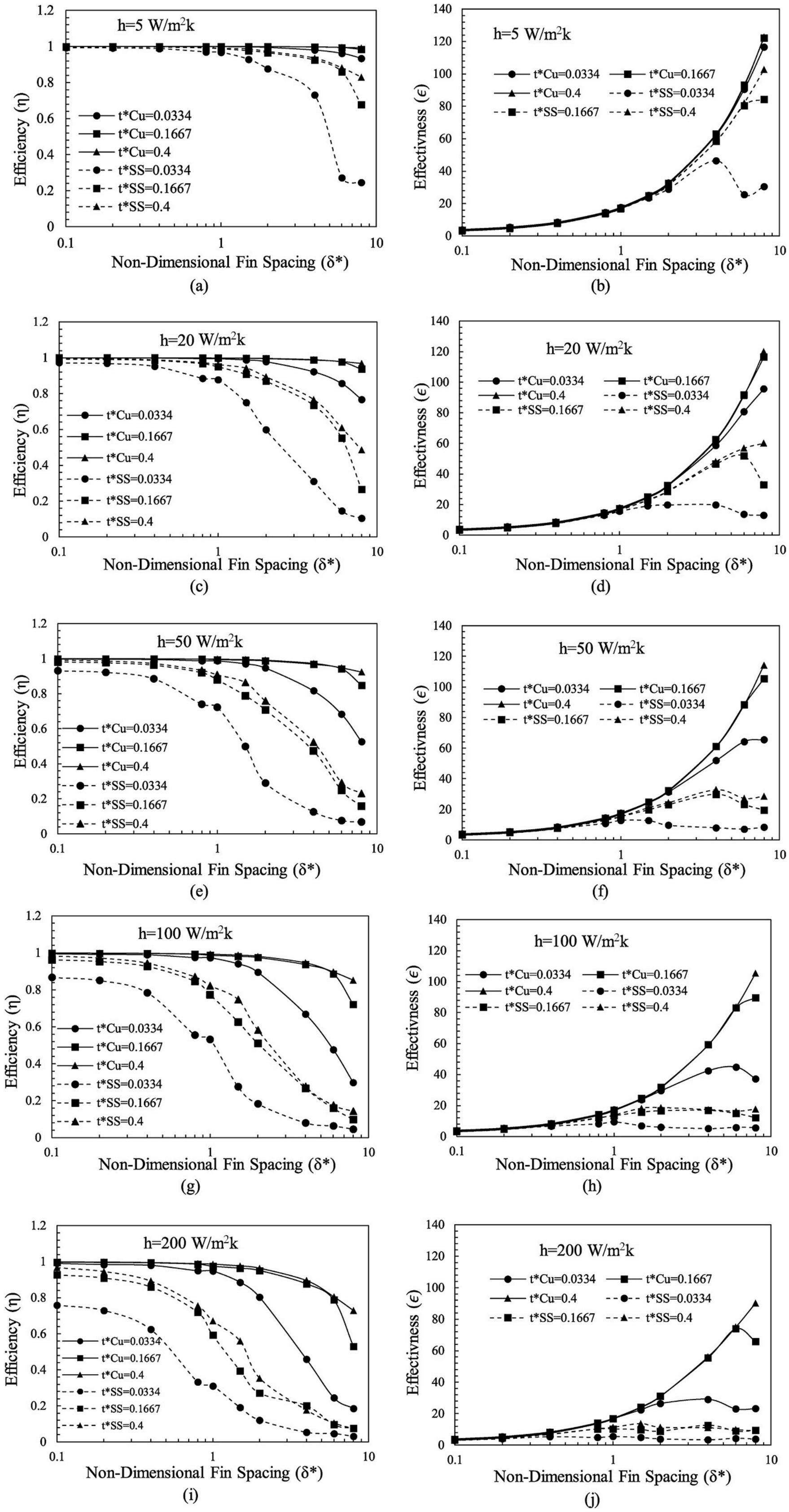

(caption on next page)

Fig. 6. Thermal performance of the novel finned-tube heat exchangers with respect to non-dimensional fin spacing for various non-dimensional fin thickness and convective heat transfer coefficients.

Where, y_i & p_i are the output variable and the corresponding predicted value for ith element in the data and $\overline{y}$ is the mean.

4. Results & discussion

This study provides insights which explain the variations of the overall efficiency (η) and the total effectiveness (ε) of a novel finned-tube system with respect to the fin spacing, the fin thickness, thermal conductivity of the material and the convective heat transfer coefficient. The number of parameters is reduced and converted to non-dimensional forms. Therefore, the non-dimensional fin spacing $\left(\delta^* = \frac{\delta}{D_o}\right)$, non-dimensional fin thickness $\left(t^* = \frac{t}{D_o}\right)$ & the convective heat transfer coefficient is being varied from 0.1 to 8, from 0.0333 to 0.4 and from 5 to 200 W/m^{2}K respectively for copper and steel fins. Fig. 5 shows the temperature profiles having same temperature bound for various geometrical models along with the heat flux values. It can be inferred that the system having copper material is showing more rate of heat transfer due to the fact that copper has higher thermal conductivity. The temperature gradients developed along the fin length for copper fins is lower than that for steel fins, consequently increasing the efficiency of copper fins. The drop in temperature along the fins length is increasing with the increase in fin thickness. In Fig. 6, the overall efficiency and total effectiveness of the novel finned-tube system is represented with respect to the δ^* for different values of t^*. For steel fins the decrease in fin efficiency is gradual till $\delta^* = 1$, the it is decreasing rather quickly with δ^* in contrast to copper fins. Moreover, the rate of decrease of efficiency is also directly proportional to the convective heat transfer coefficient. It can be observed that for same values of δ^* & t^*, higher values of h are showing larger decrease in the efficiency. It can be asserted that overall efficiency of finned-tube system decreases with increase in δ^* & h, and it increases with increase in t^*. The maximum efficiency $\eta_{max} = 0.99975$ is achieved at $\delta^* = 0.1$ & $t^* = 0.0133$ for $h = 5\ W/m^2.K$ with copper material. The total effectiveness of the system for copper fins is seen to be insensitive to the

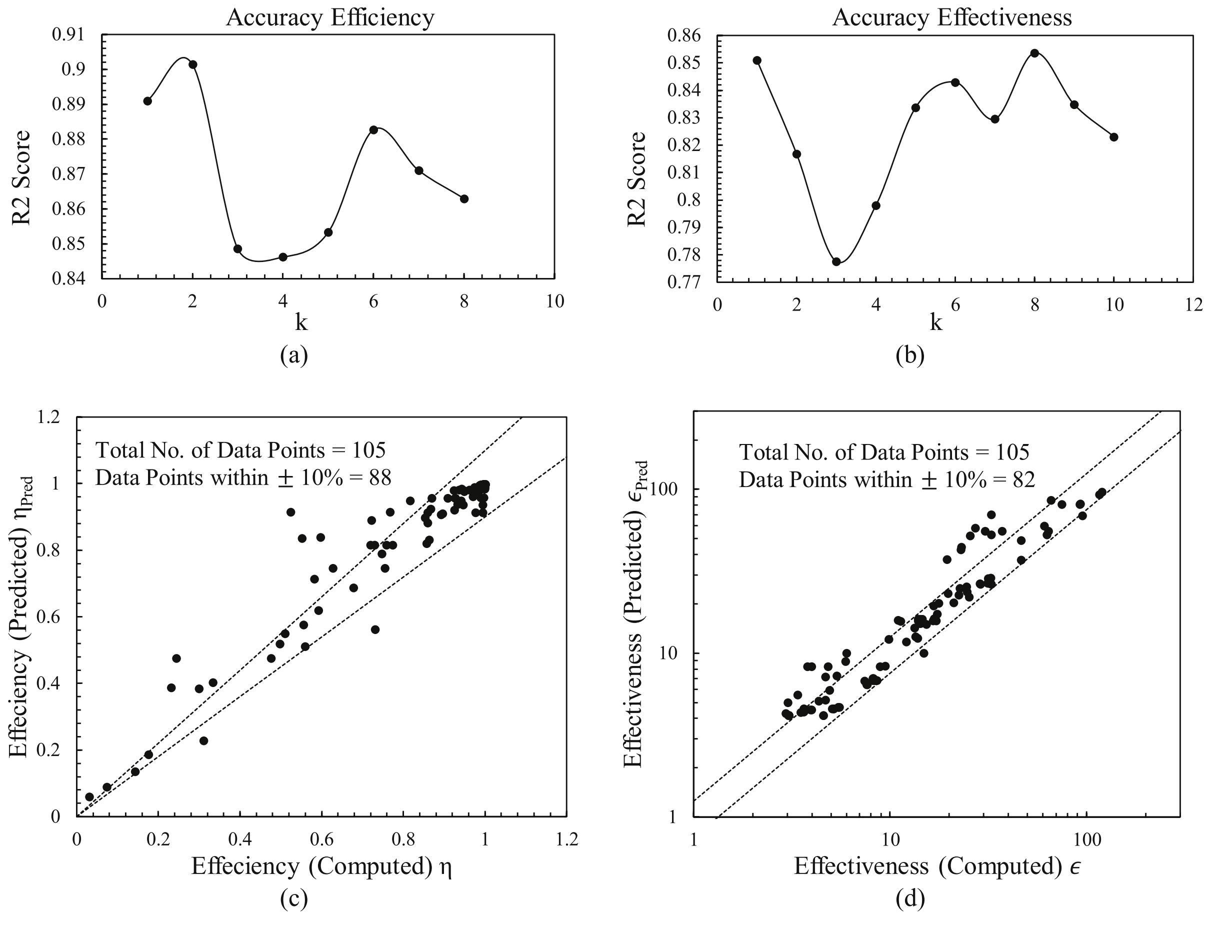

Fig. 7. Results of k-NN regression showing variation of R^2 score with k value (a & b) along with predicted and computed outputs for efficiency and effectiveness (c & d).

fin thickness for $h = 5$ & $20\ W/m^2K$, however, it is decreasing with the increase in δ^* for $h = 50, 100$ & $200\ W/m^2K$. The effectiveness of steel fins is observed to be decreasing with δ^* for all values of *h*. It can be concluded that the total effectiveness is increasing with increase in δ^* & t^* and is decreasing with *h*. The maximum effectiveness $\varepsilon_{max} = 122.766$ is for $\delta^* = 8$ & $t^* = 0.4$ for $h = 5\ W/m^2.K$.

The variation of R^2 values with "*k*" has been recorded and presented in Fig. 7 and it is clear that $k = 2$ is predicting the highest accuracy for Efficiency and $k = 8$ is giving the highest accuracy for Effectiveness predictions. The R^2 value for efficiency at k = 2 is 0.9014 and for effectiveness at k = 8 is 0.8537, which implies that the regression model predictions are in good agreement with the actual computed outputs as shown in Fig. 7 c & d. It can be observed that for Efficiency, 88 out of 105 data points are lying within the 10% error range and for effectiveness, 85 out of 105 data points are lying with the 10% error range. The *k*-NN regression algorithm is showing remarkable accuracies therefore, it is an exceptional tool for thermal system designer for predicting outputs without computationally solving the thermal system at its entirety.

5. Conclusion

The convective heat transfer coefficient (*h*) is being varied along with variation in fin geometry (δ & t) for two materials copper and steel to analyze the effects on the thermal performance of this novel finned-tube heat exchanger. It is concluded that copper is the obvious choice of material for the finned-tube system. The efficiency has direct proportionality with fin thickness and inverse proportionality with fin spacing & heat transfer coefficient. The maximum efficiency is achieved with the shortest & thickest fin for the lowest heat transfer coefficient. The effectiveness is showing direct relation with fin spacing & fin thickness and inverse relation with the heat transfer coefficient. The maximum overall effectiveness of the system is achieved for the longest and thickest fin with the lowest heat transfer coefficient. The *k*-NN regression model resulted in high prediction accuracies and because of its advantages, *k*-NN can be an extremely useful tool for thermal system design engineers.

Declaration of competing interest

The authors declare that they have no known competing financial interests or personal relationships that could have appeared to influence the work reported in this paper.

CRediT authorship contribution statement

Gaurav Krishnayatra: Data curation, Conceptualization, Writing - original draft. **Sulekh Tokas:** Conceptualization, Writing - review & editing. **Rajesh Kumar:** Supervision, Writing - review & editing.

Nomenclature

D_o	Outer diameter of the tube, m
D_i	Inner diameter of the tube, m
δ	Fin spacing, m
L_f	Length of fin, m
t	Thickness of fin, m
T	Temperature (general), $^\circ C$
T_w	Temperature of inner wall, $^\circ C$
T_∞	Temperature of the free stream, $^\circ C$
L	Axial length of the hollow cylinder, m
t^*	Non-dimensional fin thickness, $t^* = t/D_o$
δ^*	Non-dimensional fin spacing, $\delta^* = \delta/D_o$
A_t	Total surface area, m^2
h	Convective heat transfer coefficient, $W/m^2.K$
q	Heat transfer per unit area, simulations result, W/m^2
Q	Total rate of heat transfer, W, $Q = \frac{(T_w - T_\infty)}{\frac{\ln\left(D_o/D_i\right)}{2\pi kL} + \frac{1}{\eta_o A_t h}}$
k_{ss}	Thermal conductivity of Steel, $W/m.K$
k_{cu}	Thermal conductivity of Copper, $W/m.K$
k	Thermal conductivity (general), $W/m.K$
η_o	Overall Efficiency of finned-tube system, $\eta_o = 1 - \frac{NA_f}{A_t}(1 - \eta_f)$
η_f	Efficiency of single fin
N	Number of Fins
A_f	Area of single fins, m^2
L_{exp}	Outer surface perimetric length of the finned-tube system, m, $L_{exp} = 112\delta + 16(D_o - t)$

η	Efficiency computed by computational results, $\eta = \frac{q}{h(T_w - T_\infty)}$
ε	Effectiveness computed by computational results, $\varepsilon = \frac{Q}{hA_o(T_w - T_\infty)}$
M	Non-dimensional parameter "M", $M = \frac{h}{8k}L_{exp}$
η_{pred}	Predicted Efficiency
ε_{pred}	Predicted Effectiveness
η_{max}	Maximum value of the Efficiency
ε_{max}	Maximum value of the Effectiveness
d_{ij}	Euclidean distance between ith and jth elements of the predictors, $d_{ij} = \sqrt{(x_i - x_j)^2 + (z_i - z_j)^2}$
x_i, z_i	Predictor variables for ith element
k	Number of neighbors used in k-NN algorithm
y_i	ith Output variable used for regression
p_i	Predicted Output for ith element
R^2	R-squared values, $R^2 = 1 - \frac{\sum_i (y_i - p_i)^2}{\sum_i (y_i - \bar{y})^2}$

Appendix A. Supplementary data

Supplementary data to this article can be found online at https://doi.org/10.1016/j.csite.2020.100706.

References

[1] A.D. Kraus, A. Aziz, J. Welty, Extended Surface Heat Transfer, John Wiley & sons, 2001.
[2] N. Nagarani, K. Mayilsamy, A. Murugesan, G.S. Kumar, Review of utilization of extended surfaces in heat transfer problems, Renew. Sustain. Energy Rev. 29 (2014) 604–613, https://doi.org/10.1016/j.rser.2013.08.068.
[3] D.R. Harper, W.B. Brown, Mathematical Equations for Heat Conduction in the Fins of Air Cooled Engines, vol. 158, National Advisory Committee on Aeronautics, Washington, DC, 1922. NACA Rep. https://ntrs.nasa.gov/search.jsp?R=19930091223.
[4] E. Schmidt, Die warmeuebertragung durch rippen, Z. Des. Vereines Dtsch. Ingenieure 70 (1926) 885–951.
[5] P.J. Heggs, T.H. Ooi, Design charts for radial rectangular fins in terms of performance ratio and maximum effectiveness, Appl. Therm. Eng. 24 (2004) 1341–1351, https://doi.org/10.1016/j.applthermaleng.2003.12.021.
[6] A. Alam, P.S. Ghoshdastidar, A study of heat transfer effectiveness of circular tubes with internal longitudinal fins having tapered profiles, Int. J. Heat Mass Tran. 45 (2002) 1371–1376, https://doi.org/10.1016/S0017-9310(01)00240-X.
[7] N. Nagarani, K. Mayilsamy, A. Murugesan, G.S. Kumar, Review of utilization of extended surfaces in heat transfer problems, Renew. Sustain. Energy Rev. 29 (2014) 604–613, https://doi.org/10.1016/j.proeng.2012.06.343.
[8] P.M. Cuce, E. Cuce, Optimization of configurations to enhance heat transfer from a longitudinal fin exposed to natural convection and radiation, Int. J. Low Carbon Technol. 9 (2014) 305–310, https://doi.org/10.1093/ijlct/ctt005.
[9] A. Aziz, F. Khani, Analytical solutions for a rotating radial fin of rectangular and various convex parabolic profiles, Commun. Nonlinear Sci. Numer. Simulat. 15 (2010) 1565–1574, https://doi.org/10.1016/j.cnsns.2009.07.008.
[10] R.E.K.V. Okiy, An assessment of extended surfaces-two dimensional effects, Int. J. Eng. Res. Afr. 15 (2015) 71–85. https://doi.org/10.4028/www.scientific.net/JERA.15.71.
[11] T. Samana, T. Kiatsiriroat, A. Nuntaphan, Enhancement of fins efficiency of a solid wire fin by oscillating heat pipe under forced convection, Case Studies Thermal Engg 2 (2014) 36–41, https://doi.org/10.1016/j.csite.2013.10.003.
[12] W. Li, L. Yang, J. Ren, H. Jiang, Effect of thermal boundary conditions and thermal conductivity on conjugate heat transfer performance in pin fin arrays, Int. J. Heat Mass Tran. 95 (2016) 579–592, https://doi.org/10.1016/j.ijheatmasstransfer.2015.12.010.
[13] M. Ramezanizadeh, M.A. Nazari, Modeling thermal conductivity of Ag/water nanofluid by applying a mathematical correlation and artificial neural network, Int. J. Low Carbon Technol. 14 (2019) 468–474, https://doi.org/10.1093/ijlct/ctz030.
[14] A. Maleki, A. Haghighi, M.I. Shahrestani, Z. Abdelmalek, Applying different type of artificial neural network for modelling thermal conductivity of nanofluids containing silica particles, J. Therm. Anal. Calorim. (2020), https://doi.org/10.1007/s10973-020-09541-x.
[15] P. Harrington, Machine Learning in Action, Manning Publications Co., New York, USA, 2012.
[16] N.S. Altman, An introduction to kernel and nearest-neighbor nonparametric regression, Am. Statistician 46 (1992) 175–185, https://doi.org/10.1080/00031305.1992.10475879.